

Inhibited carrier transfer in ensembles of isolated quantum dots

C. Lobo

Department of Electronic Materials Engineering, Research School of Physical Sciences and Engineering, Australian National University, Canberra ACT 0200 Australia

R. Leon

Jet Propulsion Laboratory, California Institute of Technology, Pasadena CA 91109

S. Marcinkevičius

Department of Physics-Optics, Royal Institute of Technology, S-100 44 Stockholm, Sweden

W. Yang and P. C. Sercel

Department of Physics and Materials Science Institute, University of Oregon, Eugene OR

X. Z. Liao, J. Zou and D. J. H. Cockayne

Australian Key Centre for Microscopy and Microanalysis, Electron Microscopy Unit, University of Sydney, Sydney NSW 2006 Australia

We report significant differences in the temperature dependent and time-resolved photoluminescence (PL) from low and high surface density InGaAs/GaAs quantum dots (QDs). QDs in high densities are found to exhibit an Arrhenius dependence of the PL intensity, while low-density (isolated) QDs display non-Arrhenius behaviour. The PL temperature dependence of high density QD samples is attributed to carrier thermal emission and recapture into neighbouring QDs. Conversely, in low density QD samples, thermal transfer of carriers between neighbouring QDs plays no significant role in the PL temperature dependence. The efficiency of carrier transfer into isolated dots is found to be limited by the rate of carrier transport in the InGaAs wetting layer. These interpretations are consistent with time-resolved PL measurements of carrier transfer times in low and high density QDs.

I. INTRODUCTION

Time-resolved and temperature-dependent photoluminescence (PL) measurements of quantum dot (QD) ensembles have helped to clarify the processes of energy relaxation and energy transfer in multiple and coupled quantum dot systems.¹⁻⁵ However, the influence of dot size and density on the luminescence energies and linewidths from QD ensembles is still not well understood, and the mechanisms involved in carrier relaxation and PL quenching seem strongly dependent on the material system, excitation conditions, and method of QD formation (self-assembled or strain-induced). It has recently been reported that the PL emission energies, inhomogeneous linewidths, intersublevel energies, and excited state relaxation times of ensembles of InGaAs/GaAs QDs are strongly influenced by the QD density.⁶ Here we have investigated the luminescence emission from low density and high density $\text{In}_x\text{Ga}_{1-x}\text{As}/\text{GaAs}$ QDs by temperature-dependent and time-resolved PL. We find that the temperature dependence of the PL emission is determined primarily by the efficiency of carrier thermal transfer into the QDs. We also report differences in the degree of linewidth broadening of the PL emission from these low and high density QDs as a function of temperature. These differences result from the reduced influence of thermally activated carrier transfer and strain interac-

tion as the average dot separation increases.

II. EXPERIMENTAL METHODS

QD structures of nominal composition $\text{In}_{0.6}\text{Ga}_{0.4}\text{As}$ were grown on slightly misoriented, semi-insulating GaAs(100) substrates by metal organic chemical vapour deposition (MOCVD) in a horizontal reactor cell operating at 76 Torr. The structures were grown under identical conditions, except for the AsH_3 partial pressure, which was varied in order to obtain widely differing densities of similar-sized InGaAs islands.⁷ QD samples used for photoluminescence measurements were capped with 100 nm GaAs. Full details of the growth conditions are given in Ref. [7].

Average dot sizes in the capped samples used for PL measurements were determined by plan-view transmission electron microscopy (TEM) using a Phillips EM430 operating at 300 keV. Island concentrations were determined both by TEM of capped samples and by atomic force microscopy (AFM) of uncapped QD samples grown under identical conditions to the capped samples used for PL. Temperature dependent PL measurements were undertaken with above-bandgap excitation using a Ti:sapphire laser emitting at 804 nm pumped by an Argon ion laser ($\lambda = 488\text{nm}$), or directly using an Argon

ion laser. The signal was dispersed by a 0.25 m single grating monochromator and collected using a liquid N₂ cooled Germanium detector. QD samples were mounted with Indium to prevent sample heating. The average excitation power was 1 W/cm².

Carrier transfer times into the QDs were measured by time-resolved photoluminescence (TRPL) in the temperature range 80 - 300 K. A self mode-locking Ti:sapphire laser (80 fs, 95 MHz, 800 nm) was used for excitation, and an upconversion technique with a temporal resolution of 150 fs used for signal detection. Excitation powers varied in the range 0.01 to 10 mW. The average excitation intensity for the temperature-dependent measurements was 10 W/cm², which corresponds to approximately 2×10^{11} electron-hole pairs per square centimetre when spot size and reflections are taken into account.

III. TEMPERATURE-DEPENDENT PHOTOLUMINESCENCE

Figure 1 shows plan-view TEM and AFM images of representative high and low density QD samples. The low-density QD samples A and B (shown in Fig. 1(a) and 1(c) respectively) have nominal miscut angles of 0.25° and 0.75° off the (100) plane. These samples have dot densities of approximately 3.5×10^8 cm⁻² and 7×10^8 cm⁻². Average (edge to edge) QD separations are 280 nm in sample A and 190 nm in sample B. The high density QD sample shown in Fig. 1(b) and 1(d) is nominally on-axis $[(100) \pm 0.05^\circ]$ and has an average dot density of 2.5×10^{10} cm⁻² and an average QD separation of 10 nm. The average diameter of dots in all three capped samples is (25 ± 5) nm.

Low-temperature PL spectra from high and low density QDs are displayed in Fig. 2. Emission from the ground state and two excited states is observed from the low-density sample even under conditions of low excitation. This may be due to hindered intersublevel relaxation.⁸⁻¹⁰ In contrast, the high density QDs show only ground state emission under continuous-wave (CW) excitation. The lineshape of the PL emission from high density QDs is unchanged with increasing excitation power.⁶ The high-density dots also exhibit a blueshift of the PL emission energy and a broadening of the ground state inhomogeneous linewidth with respect to the low-density QDs at the same low temperature. These differences have been ascribed to progressive strain deformation of the QD confining potentials which effectively result in shallower confinement as the dot density increases.⁶ The increased degree of strain interaction between neighbouring high-density QDs, together with the randomness of these interactions, account for the observed differences in the CW PL. From here on these low and high density QDs will therefore be referred to as ‘isolated’ and ‘interacting’ respectively.

A. Interacting QDs

The normalised PL intensity from interacting QDs is plotted as a function of temperature in Fig. 3. These QDs exhibit the Arrhenius behaviour typically observed for quantum wells^{11,12} (see inset, Fig. 3). The activation energy E_A extracted from these Arrhenius plots approximates the energy difference between the QD emission and that of the wetting layer (WL) or barrier. Emission from the WL in interacting QD samples is absent except at very low temperatures (< 20 K) or under high excitation densities. Reported observations of a large increase in QD luminescence when the excitation energy exceeds the WL emission energy,¹³ and of an increase in the WL/QD intensity ratio with excitation power¹⁰ indicate that carriers are generated in the WL (and GaAs barrier) and subsequently transferred to the QDs. Hence the lack of WL emission in CW PL indicates rapid carrier transfer from the WL to the high-density QDs.

The temperature dependencies of the PL redshift and inhomogeneously broadened linewidth (Full Width at Half Maximum, FWHM) of the QD emission are plotted in Fig. 4. The QD PL redshift is significantly greater than that of the InGaAs free exciton emission¹⁹ at temperatures above 100K. The FWHM of the QD PL emission first decreases and then increases over an 8 meV range with increasing temperature. Similar dependencies of the energy shift and FWHM of the QD PL peak on temperature have been reported previously¹⁶⁻¹⁸ and attributed to the effects of thermal activation transfer and tunnelling transfer between neighbouring QDs (see Fig. 5). At low temperatures, there is no significant thermal emission of carriers out of the QDs. Hence the PL redshift of the QD peak is equivalent to that of the InGaAs bandgap and the FWHM remains constant. Above ≈ 100 K, carrier thermal emission out of the smaller QDs in the ensemble and recapture by neighbouring QDs with deeper confining potentials becomes significant. This behaviour explains the simultaneous redshifting and narrowing of the PL peak. At higher temperatures (above ≈ 150 K) the FWHM increases and the rate of redshift decreases as thermal emission of carriers out of the larger QDs in the ensemble becomes significant. Tunnelling of carriers between neighbouring QDs may also play a role, although this process is independent of temperature and would lead to a reduction of the FWHM across the whole temperature range. Attempts to model the observed behaviour by accounting only for carrier thermal transfer between neighbouring QDs have been only partially successful.^{16,17} In particular the FWHM at high T is often greater than that at low T, an observation that cannot be explained by a simple thermionic emission model. A successful model may require inclusion of the effects of alloy broadening and varying strain interactions between neighbouring QDs.

B. Isolated QDs

PL emission from the ground and excited states of the isolated QDs can be modelled by Gaussians with a constant inhomogeneous broadening factor (Γ = FWHM) and level spacings of 45 - 50 meV.¹⁰ The integrated PL intensity, energy shift, and FWHM extracted from these fits to the PL spectra are plotted as a function of temperature in Figures 3 and 4. The integrated intensity of the luminescence emission from the ground and excited states increases from 20 - 90 K, and subsequently decreases up to 210 K (see Fig. 3). The total PL intensity at 90 K is approximately twice the low-temperature value. At low temperature, the wetting layer (WL) emission is more intense than the QD emission. The integrated intensity of the WL emission as a function of temperature is also plotted in Fig. 3. This plot shows that the wetting layer emission obeys the Arrhenius dependence observed for quantum wells.^{11,12}

Wetting layer emission spectra obtained at a number of temperatures are shown in Fig. 6. The lineshape of the broad WL emission changes with increasing temperature. The intensity of the low-energy tail increases relative to the high-energy tail, indicating the existence of potential fluctuations in the WL. Such fluctuations may be caused by Indium segregation and enrichment in the quantum dots,¹⁴ which would produce Gallium-rich regions in the WL. Variations in strain induced by the QDs would also produce regions of lateral confinement in the WL.¹⁰ The observed change in the lineshape of the WL emission with increasing temperature indicates that some carriers thermally emitted from regions of the WL with shallow confining potentials are retrapped and recombine in regions of deeper confinement. This behaviour is analogous to retrapping of carriers thermally emitted from shallow wells by adjacent deeper wells in multiple quantum well samples.¹⁵

It has been established that carrier transfer to these InGaAs/GaAs quantum dots occurs via the WL.^{10,13} The WL behaves as a reservoir of carriers, available to the QDs provided the 2D diffusion length in the WL is long enough for capture into the QDs to occur prior to recombination in the WL. In high-density QDs, the absence of a WL emission in CW PL indicates that the average dot-dot separation is shorter than the carrier diffusion length in the WL.¹⁰ The carrier mobility in the WL would be expected to play a greater role in the rate of carrier transfer to the QDs as the average dot-dot separation increases.

We attribute the increase in PL intensity from isolated QDs (Fig. 3) to carrier transfer mechanisms in the WL. At elevated temperatures, carriers trapped at potential fluctuations in the WL may acquire sufficient thermal energy to overcome these barriers. Such an increase in carrier thermal transfer within the WL would result in an increased rate of carrier capture by the QDs and produce the observed increase in QD PL intensity. The rate of carrier transfer to the QDs is also limited by the rate of

lateral transport in the InGaAs WL, which for photoexcited carriers is governed by hole diffusion. Hole mobility in InGaAs increases with temperature up to ≈ 100 K.²⁰ This increase in hole mobility may increase the rate of carrier capture into the QDs and therefore contribute to the observed increase in QD PL intensity. At temperatures greater than 100 K, thermal emission of carriers from the QDs becomes dominant. The QD PL intensity therefore follows an approximately exponential decrease up to room temperature.

The PL redshift of the emission from the ground state and first excited state of the isolated QDs is plotted as a function of temperature in Fig. 4. The redshift of both emissions follows that of the InGaAs free exciton emission with increasing temperature. The inhomogeneously broadened linewidth of the isolated QDs shows an approximately linear decrease from 45 to 41 meV over the temperature range 10 - 210 K. We attribute these behaviours to thermal emission of carriers from the smaller QDs in the ensemble without subsequent recapture by larger QDs. Thus carrier transfer between neighbouring QDs has no significant effect on the PL temperature dependence.

IV. TIME-RESOLVED PHOTOLUMINESCENCE

Carrier transfer in isolated and interacting quantum dot samples was also investigated by time-resolved photoluminescence. The rise times of the luminescence emission from the isolated and interacting QDs have been studied as a function of excitation intensity and temperature (see Fig. 7). These rise times were measured at the ground state PL peak energies, and account for carrier transport, capture and relaxation in the QDs. Fast carrier transfer into the interacting QDs is confirmed by the short PL rise times shown in Fig. 7. The rise times for interacting QDs show a slight decrease with increasing excitation power and display no significant dependence on temperature. The magnitudes and behaviour of the PL rise times for interacting QDs are very similar to those observed for quantum wells of similar composition.²³

For the isolated QDs, the PL rise times decrease from 15 to 5 ps with increasing excitation power from 0.01 to 10 mW, and increasing temperature from 80 to 300 K. The excitation power dependence may be explained by a reduced importance of diffusion limited transport at high carrier densities. As the excitation power increases, a greater number of carriers are generated in the vicinity of the isolated QDs. Hence the PL rise time of the isolated QDs approaches that of the interacting QDs at very high excitation densities. Potential barriers around the isolated QDs induced by band bending²¹ would also be reduced at high carrier densities due to screening of the internal electric field.²² The decrease of the PL rise time with temperature is consistent with an increased rate of carrier transfer due to carriers having greater thermal

energy to overcome these potential barriers around the QDs or in the WL.

The temperature and excitation power dependence of the rise times of the PL emission from isolated QDs confirm the interpretation of the PL temperature dependence in terms of carrier transfer mechanisms in the WL. Further studies will be undertaken on InAs QDs, in which the effects of Indium segregation and enrichment in the QDs and associated compositional fluctuations in the WL would be minimised. Differences in the PL temperature dependence of InGaAs/GaAs and InAs/GaAs QDs may clarify the effects of temperature-dependent hole mobility and potential fluctuations in the WL on carrier transfer to isolated quantum dots.

V. CONCLUSION

In conclusion, we have conducted a study of the temperature-dependent and time-resolved PL from interacting and isolated InGaAs quantum dots. We find that for high-density QD samples, the temperature dependence of the PL emission is determined by carrier thermal emission and recapture into neighbouring QDs. In low-density QDs the efficiency of carrier transfer into the dots is limited by the rate of carrier transport in the InGaAs wetting layer. Thermal transfer of carriers between neighbouring QDs plays no significant role in the PL temperature dependence.

VI. ACKNOWLEDGMENTS

C.L. thanks C. Jagadish for helpful discussions. Part of this work was sponsored by the Australian Research Council and by the Jet Propulsion Laboratory, under a contract with the National Aeronautics and Space Administration.

-
- ¹ G. Wang, S. Fafard, D. Leonard, J. E. Bowers, J. L. Merz, and P. M. Petroff, *Appl. Phys. Lett.* **64**, 2815 (1994).
² S. Raymond, S. Fafard, P. J. Poole, A. Wojs, P. Hawrylak, S. Charbonneau, D. Leonard, R. Leon, P. M. Petroff, and J. L. Merz, *Phys. Rev. B* **54**, 11548 (1996).

- ³ W. Yang, R. Lowe-Webb, H. Lee, and P. C. Sercel, *Phys. Rev. B* **56**, 13314 (1997).
⁴ M. Braskén, M. Lindberg, M. Sopanen, H. Lipsanen, and J. Tulkki, *Phys. Rev. B* **58**, R15993 (1998).
⁵ Y. Zhang, M. D. Sturge, K. Kash, B. P. van der Gaag, A. S. Gozdz, L. T. Florez, and J. P. Harbison, *Superlattices and Microstructures* **17**, 201 (1995), and *Phys. Rev. B* **51**, 13303 (1995).
⁶ R. Leon, S. Marcinkevičius, X. Z. Liao, J. Zou, D. J. H. Cockayne, and S. Fafard, *Phys. Rev. B* **60** (to be published).
⁷ R. Leon, C. Lobo, J. Zou, T. Romeo, and D. J. H. Cockayne, *Phys. Rev. Lett.* **81**, 2486 (1998).
⁸ H. Benisty, C. M. Sotomayor-Torrès, and C. Weisbuch, *Phys. Rev. B* **44**, 10945 (1991).
⁹ U. Bockelmann, *Phys. Rev. B* **48**, 17637 (1993).
¹⁰ R. Leon, S. Fafard, P. G. Piva, S. Ruvimov, and Z. Liliental-Weber, *Phys. Rev. B* **58**, R4262 (1998).
¹¹ J. D. Lambkin, D. J. Dunstan, K. P. Homewood, L. K. Howard, and M. T. Emeny, *Appl. Phys. Lett.* **57**, 1986 (1990).
¹² G. Bacher, H. Schweizer, J. Kovac, A. Forchel, H. Nickel, W. Schlapp, and R. Lösch, *Phys. Rev. B* **43**, R9312 (1991).
¹³ S. Fafard, D. Leonard, J. L. Merz, and P. M. Petroff, *Appl. Phys. Lett.* **65**, 1388 (1994).
¹⁴ X. Z. Liao, J. Zou, D. J. H. Cockayne, R. Leon, and C. Lobo, *Phys. Rev. Lett.* **82**, 5148 (1999).
¹⁵ M. Vening, D. J. Dunstan, and K. P. Homewood, *Phys. Rev. B* **48**, 2412 (1993).
¹⁶ S. Fafard, S. Raymond, G. Wang, R. Leon, D. Leonard, S. Charbonneau, J. L. Merz, P. M. Petroff, and J. E. Bowers, *Surface Science* **362**, 778 (1996).
¹⁷ Z. Y. Xu, Z. D. Lu, Z. L. Yuan, X. P. Yang, B. Z. Zheng, J. Z. Xu, W. K. Ge, Y. Wang, J. Wang, and L. L. Chang, *Superlattices and Microstructures* **23**, 381 (1998).
¹⁸ A. Patané, M. Grassi Alessi, F. Intonti, A. Polimeni, M. Capizzi, F. Martelli, M. Geddo, A. Bosacchi, and S. Franchi, *Phys. Stat. Sol. A* **164**, 493 (1997).
¹⁹ S. Paul, J. B. Roy, and P. K. Basu, *J. Appl. Phys.* **69**, 827 (1991).
²⁰ The hole mobility in InGaAs peaks between 70 and 100 K, depending on the relative contributions of ionized impurity scattering, polar optical phonon scattering, acoustic phonon scattering, and alloy scattering (see S. Adachi, *Physical Properties of III-V Semiconductor Compounds*, John Wiley and Sons, 1992).
²¹ B. K. Ridley, *Phys. Rev. B* **50**, 1717 (1994).
²² G. C. Crow and R. A. Abram, *Semicond. Sci. Technol.* **14**, 1 (1999).
²³ S. Marcinkevičius and R. Leon, *Phys. Rev. B* **59**, 4630 (1999).

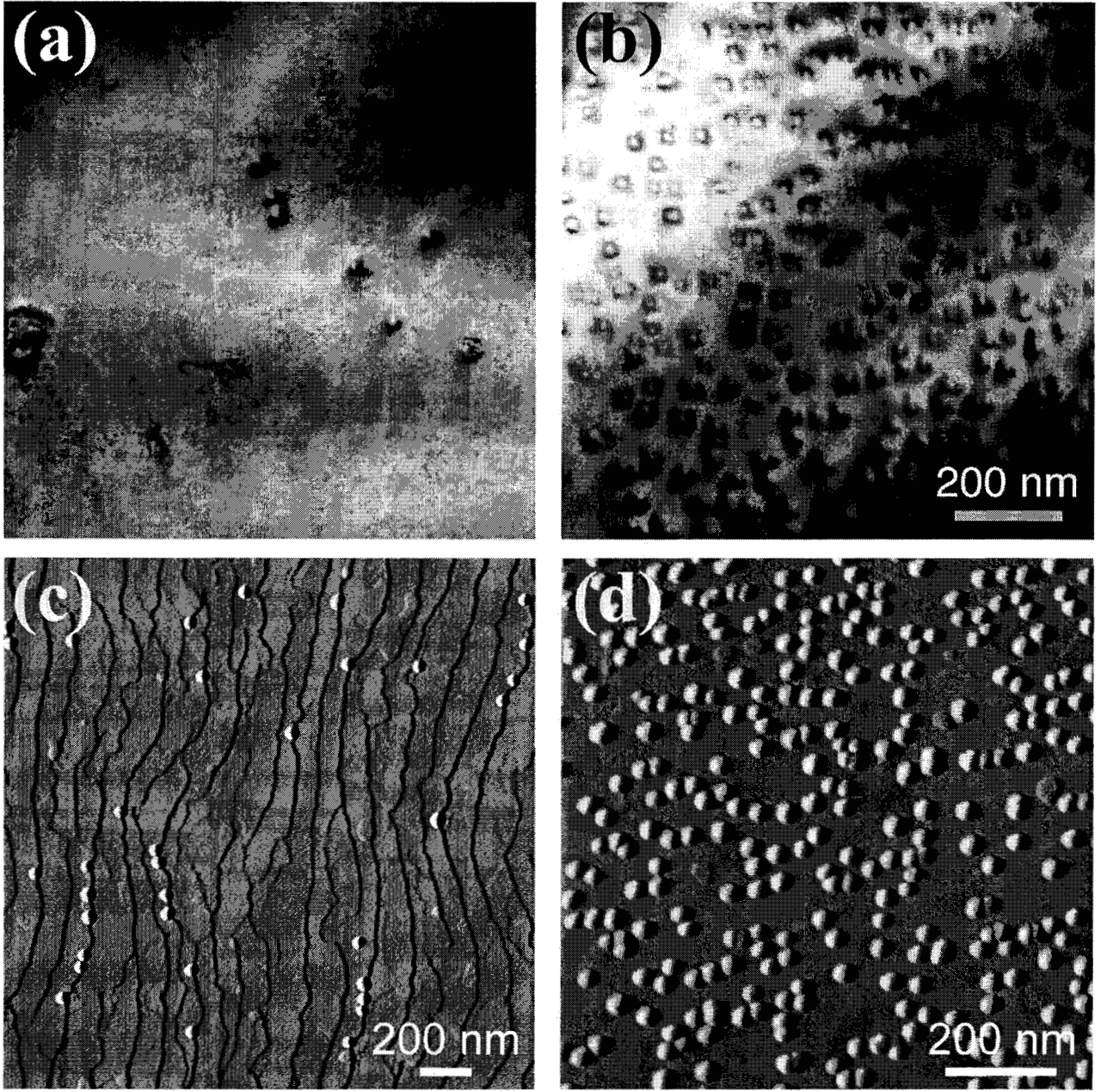


FIG. 1. Plan-view TEM images of capped samples used for PL measurements, and AFM images of uncapped samples grown under identical conditions. (a) Plan-view TEM image of isolated QDs with density $3.5 \times 10^8 \text{ cm}^{-2}$ (sample A). (b) Plan-view TEM image of interacting QDs with density $2.5 \times 10^{10} \text{ cm}^{-2}$. The scale applies to both TEM images. (c) $2 \times 2 \mu\text{m}^2$ AFM deflection image of isolated QDs with density $7 \times 10^8 \text{ cm}^{-2}$ (sample B). (d) $1 \times 1 \mu\text{m}^2$ AFM deflection image of interacting QD sample shown in (b). The average size of QDs in all three capped samples is $(25 \pm 5) \text{ nm}$.

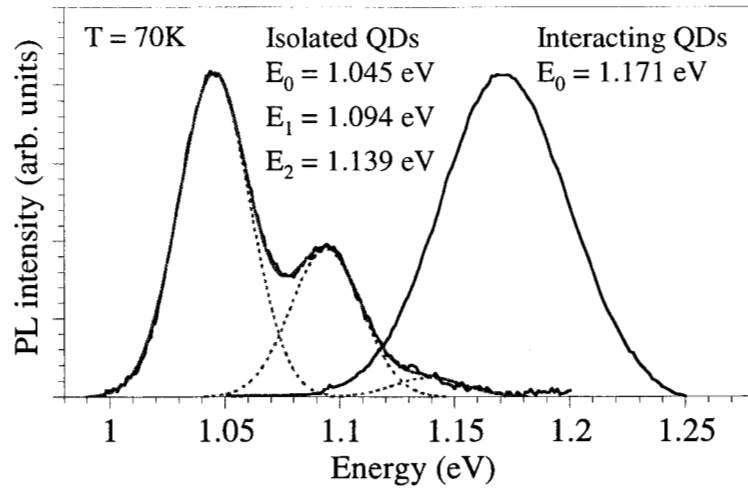


FIG. 2. Low temperature (70 K) PL spectra of isolated and interacting QDs. The spectrum from the isolated QDs (sample A) is modelled as the sum of Gaussians with peak energies $E_0 = 1.045\text{ eV}$, $E_1 = 1.094\text{ eV}$, $E_2 = 1.139\text{ eV}$ and $\Gamma = 21.8\text{ meV}$.

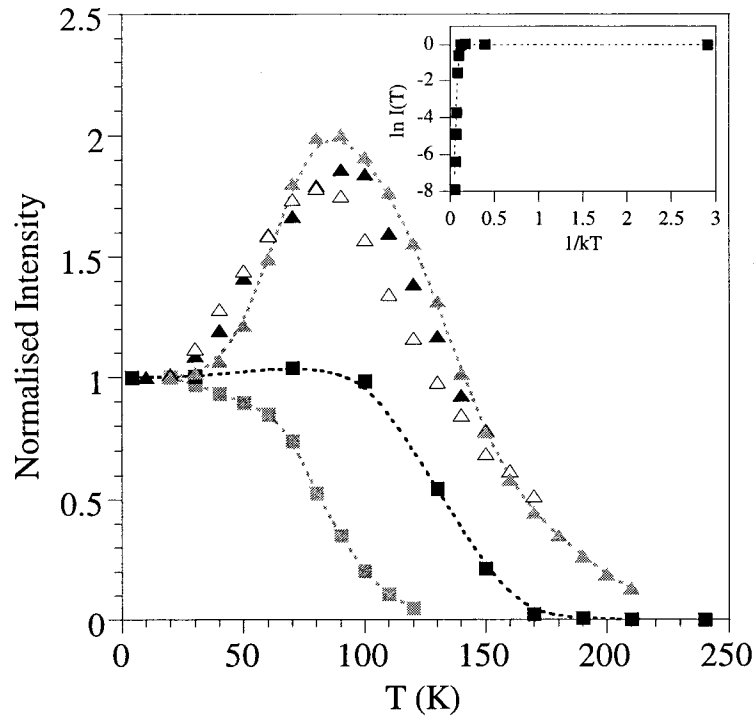


FIG. 3. Normalised integrated PL intensity as a function of temperature for several interacting and isolated QD samples. Isolated QD samples A and B are represented by filled grey and black triangles respectively; PL data from a third sample is plotted with unfilled triangles. The integrated intensity from the InGaAs WL in sample A is plotted with grey squares. PL data from the interacting QDs is plotted with black squares. The inset is an Arrhenius fit to the PL intensity from the interacting QDs as a function of temperature.

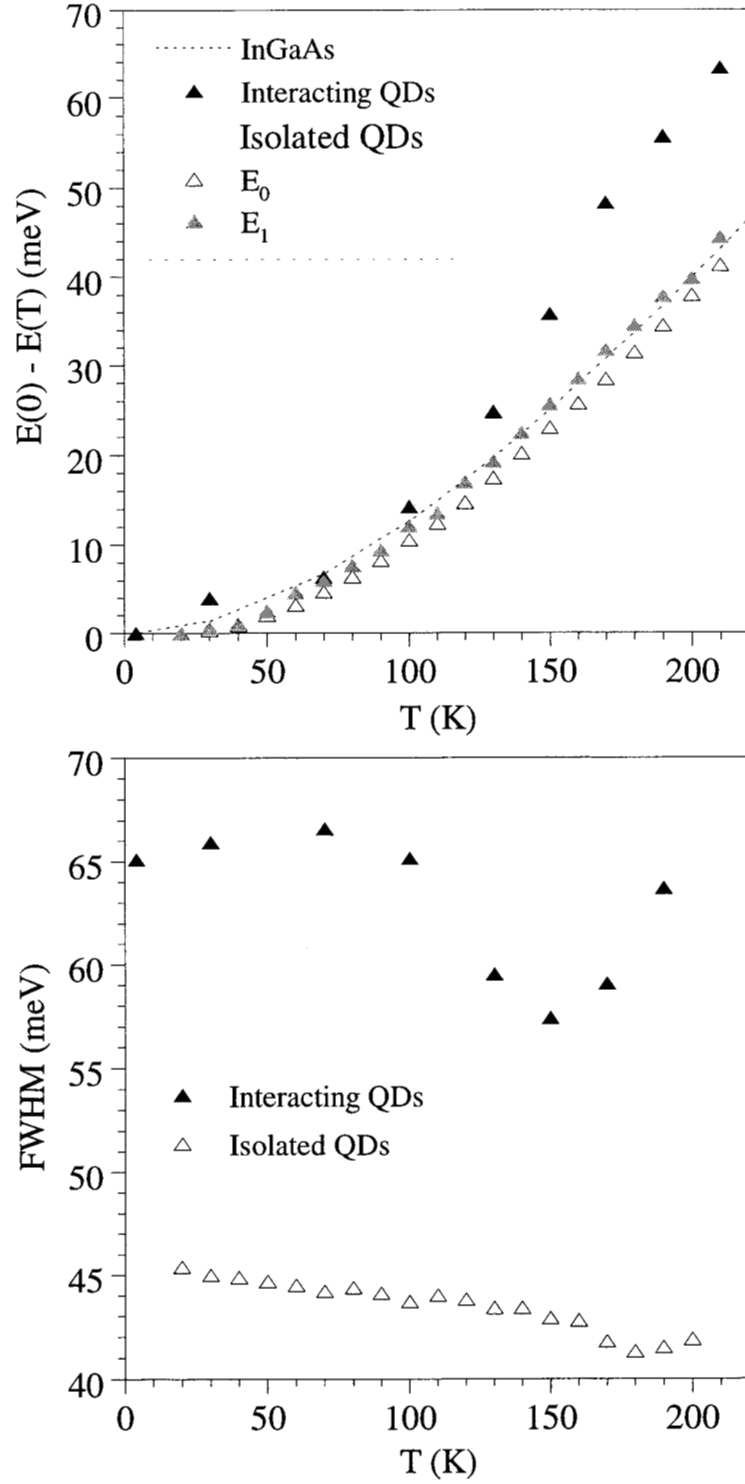


FIG. 4. (a) Redshift of the PL peak energy as a function of temperature for the interacting and isolated (sample A) QDs plotted with that of the InGaAs free exciton emission. (b) Inhomogeneous linewidth broadening (FWHM) as a function of temperature for interacting and isolated (sample A) QDs.

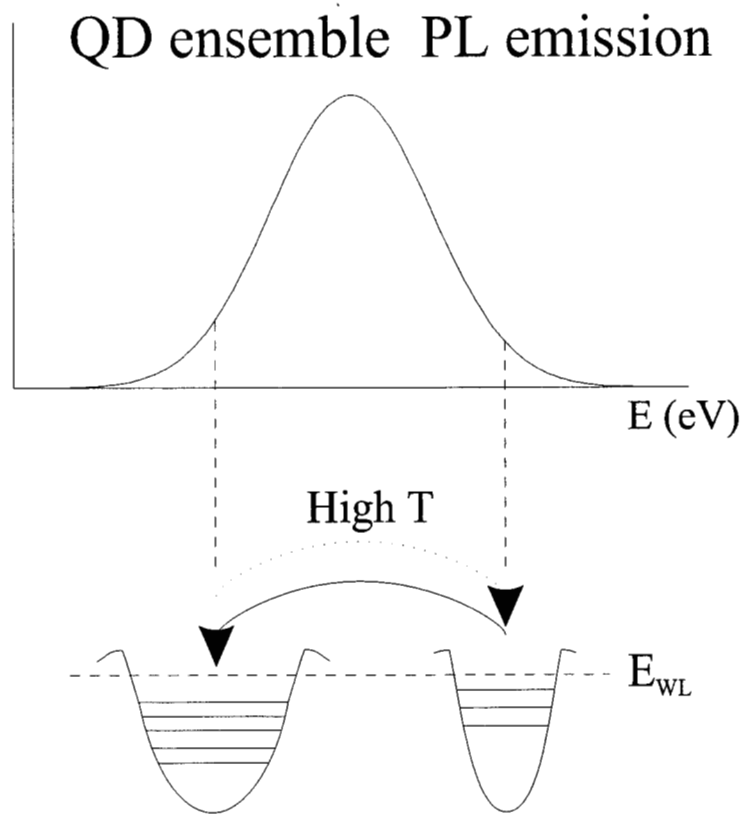


FIG. 5. Schematic of thermally activated carrier transfer between neighbouring quantum dots in high-density QD structures.

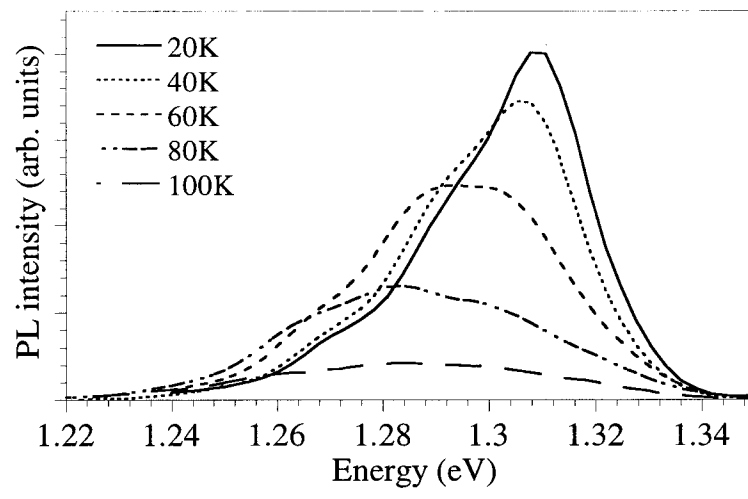


FIG. 6. Luminescence emission from the wetting layer in isolated QD sample A at several temperatures.

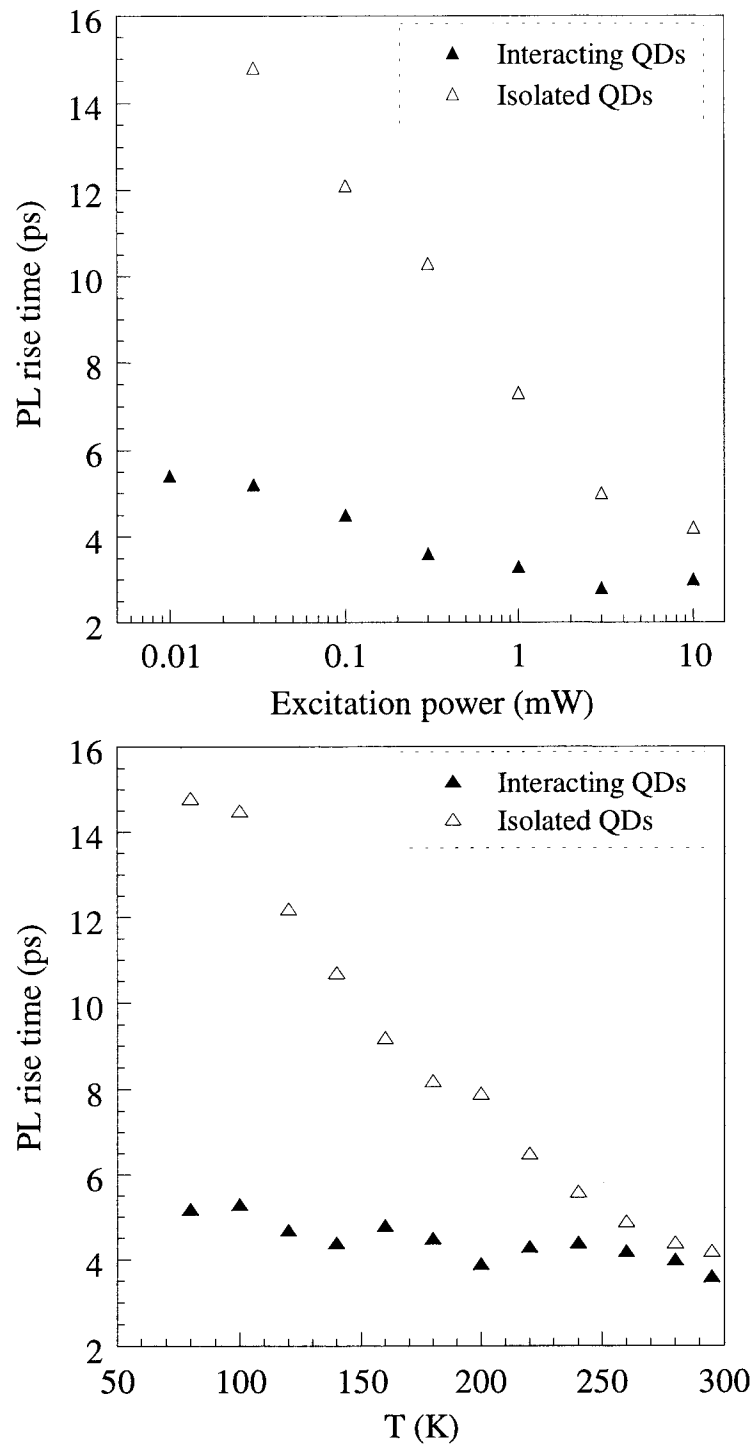


FIG. 7. PL rise times as a function of (a) excitation power and (b) temperature for interacting and isolated (sample B) QDs.